

To cite this article: Abdelouahad BAYAR (2025). TWO-DIMENSIONAL CUBIC BÉZIER CURVES INTERPOLATION OF NON-DEGENERATE SEQUENCES OF POINTS PRESERVING CONVEXITY, MONO-INFLECTION, AND OBLIQUITY, International Journal of Current Research and Applied Studies (IJCRAS) 4 (3): Article No. 123, Sub Id 217

## **TWO-DIMENSIONAL CUBIC BÉZIER CURVES INTERPOLATION OF NON-DEGENERATE SEQUENCES OF POINTS PRESERVING CONVEXITY, MONO-INFLECTION, AND OBLIQUITY**

**Abdelouahad BAYAR<sup>1</sup>**

<sup>1</sup>Department of Computer Science, PSSII Lab (Laboratoire des Processus Signaux, Systèmes Industriels et Informatique), Higher School of Technology of Safi, Cadi Ayyad University, Safi, Morocco

DOI: <https://doi.org/10.61646/IJCRAS.vol.4.issue3.123>

### **ABSTRACT**

This paper introduces a method for interpolating oblique non-degenerate sequences of points through the use of specific cubic BÉZIER curves (splines), resulting in a global curve that also preserves its obliquity. The interpolation technique employs two-dimensional BÉZIER curves that are designed to be either convex or mono-inflective. These curves ensure that their scalar functions remain monotonic, thereby maintaining the obliquity, convexity, and any inflections present in the sequence being interpolated. Furthermore, this approach can be extended to interpolate any sequence of points using oblique two-dimensional convex and mono-inflective curves, not limited to just oblique non-degenerate sequences.

**Keywords:** Interpolation, non-degenerate Sequences of Points, Two-Dimensional BÉZIER Splines, Obliquity, Convexity, Mono-Inflection.

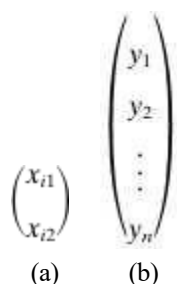


Figure 1: Parentheses (delimiters) as dynamic symbols

## INTRODUCTION

We present an algorithm designed to interpolate a non-degenerate sequence of points while maintaining monotonicity in both dimensions using a set of two-dimensional cubic BÉZIER curves. The resulting interpolating curves also preserve monotonicity in both coordinates. This article extends the work published in [3], where an interpolation approach for convex oblique point sequences was described. In this paper, we generalize the method to accommodate cases where the sequence of oblique points may be convex or exhibit inflections. Not only have we added support for inflections, but we have also significantly reformulated the mathematical framework. This research is motivated by the need for dynamic scaling of font characters represented in outline form.

In the context of an electronic document—especially a scientific one—characters can be classified as either static or dynamic. A static character remains consistent throughout the document, regardless of context; a mathematical symbol such as  $\alpha$  serves as a prime example. Conversely, dynamic symbols may vary in size (height, width, thickness) based on their context within the document. Mathematical delimiters, such as those illustrated in Figures 1a and 1b from [18], exemplify this behavior.

While the development of static fonts has reached a high level of sophistication, the support for dynamic characters—such as variable-sized mathematical symbols (parentheses, braces, etc.) and Arabic letters that utilize kashida (a mechanism for justifying Arabic text)—is still a work in progress. Ongoing research aims to address these challenges and find appropriate solutions [2, 4, 5, 13, 14].

### Statement of the problem

Our study on this topic concluded that the challenge of supporting curvilinear dynamic characters—unlike simpler line characters—primarily arises from mathematical formalization rather than from the font language itself. We identified several key points regarding the dynamism of symbols or characters in general:

The transition from the parentheses in Figure 1a to those in Figure 1b does not exhibit linear scaling. In fact, the height of the parentheses increases by more than threefold. However, this ratio does not apply to

their thickness. In the realm of font design, this method of scaling is known as optical scaling, as it aims to enhance visual appeal for the human eye. For further insights on optical scaling, please refer to [10, 16].

Finding an appropriate combination of affine transformations for the optical scaling of a set of curves that define the outline of a dynamic character can be challenging. The approach taken is to determine a series of control points that accurately represent the topology of the character. These control points are then interpolated using two-dimensional BÉZIER curves to create the outline of the area to be shaded. The dynamic character can be stretched as needed by applying suitable transformations to these points, ensuring that the topology of the outline remains intact. Note that the algorithm for stretching sequences of points is beyond the scope of this paper and has been submitted separately.

We have observed that the segments of the outline curves of a dynamic character that require stretching are monotonic in both the horizontal ( $x$ ) and vertical ( $y$ ) coordinates. We refer to these curves as oblique. Typically, these outline curves are also convex. It is crucial to maintain their obliquity and/or convexity throughout the stretching process. The primary contribution of this paper is an algorithm designed to interpolate a sequence of points while preserving these important properties.

A dynamic character in a document can have varying amounts of stretching, which may change as the document is edited. Therefore, the stretching algorithm should be efficient enough to be applied in real-time while the document is being rendered.

This method should be anchored in cubic BÉZIER curves and must uphold the principle of obliquity, ensuring the monotonicity of both the abscissas and ordinates of the points in the sequence. Additionally, it is essential to maintain the convexity properties. When processing a specific point in the sequence, the interpolation method will aim to minimize processing time by focusing on a small number of neighboring points, thereby enhancing processing locality at each point.

This interpolation method, as extension of that in [3], will be even more useful and applicable if it can accommodate not only convex sequences but also those with some inflections. This development is particularly interesting given our observations that the Persian calligraphic style we are beginning to study can exhibit inflections in its stretchable parts.

### **Prior work**

Spline interpolation has garnered significant interest over the years. Several books have been published on the subject, including works by DE BooR [7], SpATH [20], and Knott [12]. Additionally, numerous articles have addressed the topic, such as those by FRITSCH [9] and DoUGHERTY [8]. Research on spline-based interpolation continues to evolve, focusing on specific objectives within particular domains [17] or seeking to enhance optimality [6, 23].

BÉZIER curves have been utilized in the design of fonts for typographic systems, including TrueType [25], Type1 [1], CurExt [14], Al-Qalam [19], and BaYaR [4].

When certain segments of the outline curve are monotonic in the  $x$ -direction (or in the  $y$ -direction), a common approach is to interpolate the control points using a scalar spline. This involves treating that

part of the outline as the graph of a function  $y = f(x)$  (or  $x = f(y)$ ). This is the procedure followed in the references cited at the beginning [7–9, 12, 20]. In certain studies, the developed methods focused on preserving monotonicity [8,9,12] and convexity [8,9]. The approach discussed in [8,9] includes additional measures to maintain shape properties, such as modifying derivatives in cases where these shape properties have been compromised.

From the perspective of BÉZIER curves, scalar interpolation—expressed as  $y_i = f(x_i)$  or, more generally,  $y = f(x)$ —results in BÉZIER curves characterized by linear (degree 1) abscissa functions. Often, utilizing BÉZIER curves with linear abscissa functions diminishes the ability to effectively capture the outlines of a shaded area with a minimal number of curves.

This paper is organized as follows: In Section 2, we will define the concept of vector rectangles and rectangular inversions. Section 3 presents and analyzes convex and mono-inflective BÉZIER curves. In Section 4, we investigate oblique cubic BÉZIER curves. Section 5 focuses on oblique BÉZIER curves generated from specific sets of characteristic vectors and their relationship to vector rectangles. In Section 6, we describe our interpolation algorithm and explore some of its properties. Section 7 presents various applications of the method. The paper concludes with a summary of findings and future perspectives.

## VECTOR RECTANGLE - RECTANGULAR INVERSION

### Vector rectangle

Let  $T = T_x T_y$  be an oblique vector ( $T$  is oblique if  $T_x \neq 0$  and  $T_y \neq 0$ ) in  $R^2$ . The set of vectors  $R_T = \sigma T_x y T_y : 0 \leq \sigma, y \leq 1$ , is the *vector rectangle with direction* (or *diagonal*, or *base*)  $T$ .

The plane  $R^2$  minus the coordinate axes consists of four quadrants, which we will denote by  $Q_1, Q_2, Q_3,$  and  $Q_4$ , in counterclockwise order, starting with the positive quadrant (the vectors with  $x > 0$  and  $y > 0$ ). Note that each quadrant contains only oblique vectors. To each quadrant  $Q$  is associated the closed quadrant  $Q$ . The latter is  $Q$  extended by bounding half-axes. The direction vector  $T$  of any vector rectangle  $R_T$  is contained in a single quadrant. On the other hand,  $R_T$  is contained in the corresponding closed quadrant. This results in four types of vector rectangles (see Figure 2).

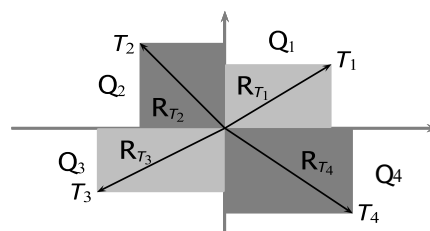


Figure 2: Quadrants and examples of vector rectangles

It's interesting to have a practical way for determining whether a vector  $U = U_x, U_y$  belongs to a vector rectangle  $R_T$ , where  $T = T_x, T_y$ . By considering the different cases based on the quadrants, we can analyze and establish the following:

$$U \in R_T \rightarrow (T_x - U_x) \cdot U_x \geq 0 \text{ and } T_y - U_y \cdot U_y \geq 0 \tag{1}$$

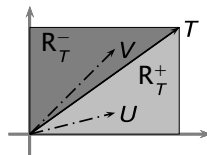


Figure 3: Positive  $R_T^+$  and negative  $R_T^-$  parts of the vector rectangle  $R_T$ ,  $U \in R_T^+$  and  $V \in R_T^-$

In this context, the notation  $U \times V$  represents the cross product of two vectors  $U$  and  $V$  in  $R^2$ , defined as the scalar  $U_x V_y - U_y V_x$ . The subsets  $R_T^+$  and  $R_T^-$  represent the two halves of the vector rectangle  $R_T$ , which are bounded by the diagonal  $D_T = \{\sigma T : \sigma \in [0, 1]\}$ . Specifically,  $R_T^+$  is the half that lies clockwise from  $T$ . Both subsets include the diagonal  $D_T$  (refer to Figure 3). When a vector  $U$  belongs to a vector rectangle  $R_T$ , this belonging is signed. The sign depends on whether  $U$  is in  $R_T^+$  or  $R_T^-$ .

We can define the subsets  $R_T^+$  and  $R_T^-$  explicitly as follows:

- $R_T^+ = \{U \in R_T : U \times T \geq 0\}$
- $R_T^- = \{U \in R_T : U \times T \leq 0\}$

It is also helpful to represent these sets in a parametric form. We have:

$$R_T^+ = rT_x, r\sigma T_y : 0 \leq \sigma, r \leq 1$$

$$R_T^- = r\sigma T_x, rT_y : 0 \leq \sigma, r \leq 1$$

Below, we state a few useful properties about vector rectangles.

**Property 1.** Let  $T = T_x, T_y$  be an oblique vector in  $R^2$ . Let  $U \in R_T$ , then we have:

- $(T - U) \in R_T$
- $T - U$  and  $U$  have opposite belonging signs with respect to  $R_T$

*Proof.*

Let  $T = T_x, T_y$  and  $U \in R_T$ .

So,  $\exists (\sigma, \gamma) \in [0, 1]^2$  such that  $U = \sigma T_x, \gamma T_y$ .

$T - U = (1 - \sigma) T_x, (1 - \gamma) T_y$ .

Then  $(T - U) \in R_T$  since  $(1 - \sigma, 1 - \gamma) \in [0, 1]^2$ .

We have  $(T - U) \times T = -U \times T$ .

Consequently,  $(T - U)$  and  $U$  have opposite belonging signs to  $R_T$ .

□

### Rectangular inversion

Rectangular inversion is a mathematical tool we have identified as essential for developing our interpolation method. This transformation is defined based on an oblique vector in  $R^2$ . While we will not provide details on how this transformation was built, we will present its definition directly.

**Definition 1** (Rectangular Inversion). Let  $T = T_x, T_y$  be a vector in  $(R^*)^2$ . We call rectangular Inversion of vector  $T$ , denoted  $\Omega_T$ , the transformation, whose associated matrix is  $M_T = \begin{pmatrix} 0 & T_x/T_y \\ T_y/T_x & 0 \end{pmatrix}$

It's easy to check that rectangular inversions meet the following interesting properties.

**Property 2.** Let  $T \in (R^*)^2$  ( $T_x \neq 0$  and  $T_y \neq 0$ ). The transformation  $\Omega_T$  designates the rectangular inversion relative to  $T$ . We have the following properties:

- (1)  $\Omega_T^2 = I_2$ ,  $I_2$  is the identity on  $R^2$ .
- (2)  $\forall U \in R_T^-$  respectively  $U \in R_T^+$ , then  $\Omega_T(U) \in R_T^+$  respectively  $\Omega_T(U) \in R_T^-$ .
- (3) Let  $Q$  be the quadrant of  $R^2$  containing  $T$ . Then we have:

- (i)  $\Omega_T(Q) = Q$  and  $\Omega_T(\overline{Q}) = \overline{Q}$ .
- (ii)  $\forall U \in \overline{Q}, U \times T = T \times \Omega_T(U)$ .

*Proof.*

#### Case Property 2(1):

Let  $T \in (R^*)^2$  and  $M_T$  be the matrix associated with the rectangular inversion  $\Omega_T$ . After calculations, we find that  $M_T^2$  is equal to the unit matrix.

#### Case Property 2(2):

We do the proof for one case and one quadrant only. It will be the same for the others.

Let  $U \in R^2$  be such that  $U \in R_T^-$ .

Assume that  $T \in Q_1$ .

$U \in R_T^-$ , so  $U = r\sigma T_x rT_y$ ,  $(r, \sigma) \in [0, 1]^2$ .

$$M_T \cdot U^t = rT_x r\sigma T_y^t$$

So  $\Omega_T(U) = rT_x r\sigma T_y$

We conclude that  $\Omega_T(U) \in R_T^+$ .

**Case Property 2(3):**

**Sub-Case Property 2(3)-(i):**

Let  $U \in Q$  resp  $U \in \bar{Q}$ .

Assume that  $U = U_x U_y$  and  $T = T_x T_y$ .

$U_x$  and  $T_x$  are of the same sign.

Also  $U_y$  and  $T_y$  are of the same sign.

$$\Omega_T(U) = \frac{T_x}{T_y} U_y, \frac{T_y}{T_x} U_x$$

We have:

$$T_x \frac{T_x}{T_y} U_y = T_x^2 \frac{U_y}{T_y} \geq 0 \text{ and } T_y \frac{T_y}{T_x} U_x = T_y^2 \frac{U_x}{T_x} \geq 0$$

Hence  $\Omega_T(U) \in Q$  res  $\Omega_T(U) \in \bar{Q}$ .

**Sub-Case Property 2(3)-(ii):**

$$\begin{aligned} T \times \Omega_T(U) &= T_x \frac{T_y}{T_x} U_x - T_y \frac{T_x}{T_y} U_y \\ &= T_y U_x - T_x U_y \\ &= U \times T \end{aligned}$$

□

## CONVEX/MONO-INFLECTIVE CUBIC BÉZIER CURVES

### Basic types

We will denote the two-dimensional BÉZIER curve with control points  $P_0, P_1, P_2$ , and  $P_3$  as  $[P_0, P_1, P_2, P_3]$ . The portion of the curve that lies within the convex hull defined by these control points is parameterized over the interval  $[0, 1]$ . The endpoints of the curve are given by  $B(0) = P_0$  and  $B(1) = P_3$ . The vectors  $U = P_1 - P_0$  and  $V = P_3 - P_2$  represent the directions of the derivatives of the curve at points  $P_0$  and  $P_3$ , respectively. The vector  $T = P_3 - P_0$  is referred to as the base of the curve.

Thus, the curve can be expressed as either  $[P_0, P_0 + U, P_3 - V, P_3]$  or alternatively as  $[P_0, P_0 + U, P_0 + T - V, T + P_0]$  when needed. Figure 4 illustrates these notations.

It is important to note that the study of the geometric characteristics of BÉZIER curves has been conducted only over the interval  $[0, 1]$ . It is well known [11, 21] that a BÉZIER curve can take various forms, such as an arch, have a single inflection point, possess two inflection points, exhibit a cusp, or form a loop (see Figure 5).

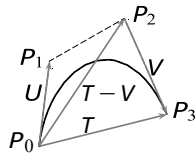


Figure 4: Point and vector characteristics of a BÉZIER curve

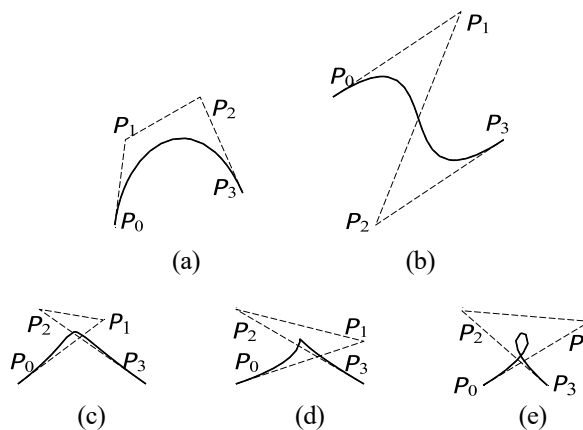


Figure 5: A two-dimensional Bézier arch (a), two-dimensional Bézier curve with one inflection point (b), two inflection points (c), a cusp (d) and a loop (e)

### Convex cubic Bézier curves

A BÉZIER arch  $[P_0, P_1, P_2, P_3]$  is defined as a curve that has non-zero curvature everywhere, although it may or may not be convex as a set of points (see Figure 6). The curve is convex if and only if the polygon  $(P_0, P_1, P_2, P_3)$  is convex. This condition can be verified by ensuring that the sign of  $(P_i - P_{i-1}) \times (P_{i+1} - P_i)$  is constant for all  $i$  from 0 to 3 (with indices evaluated modulo 4).

When the curve is expressed as  $[P_0, P_0 + U, P_0 + T - V, T + P_0]$ , convexity is guaranteed by the fact that  $U \times (T - V)$ ,  $(T - U) \times V$ ,  $U \times T$ , and  $T \times V$  all have the same sign.

Table 1: Processing details: control points and curvature function

Curve	$P_0$	$P_1$	$P_2$	$P_3$	$\Gamma(t)$
$B_a$	(10, 10)	(-20, 40)	(20, 70)	(0, 100)	$70200 \cdot t - 37800$
$B_b$	(50, 138)	(76, 165)	(56, 180)	(93, 170)	$33012 \cdot t^2 - 56142 \cdot t + 16740$
$B_c$	(20, 30)	(60, 60)	(30, 65)	(80, 30)	$86400 \cdot t^2 - 91800 \cdot t + 19800$

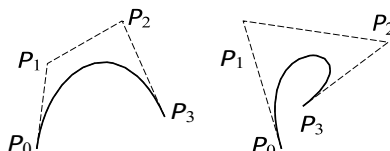


Figure 6: Convex Bézier arch (left) and non-convex Bézier arch (right)

### Mono-inflective cubic Bézier curves

The application of BÉZIER curves across various fields relies on the section of the curve that lies within the convex hull defined by its control points. From a parameterization perspective, we focus on the segment of the curve corresponding to the interval  $[0, 1]$ .

In addition to exploring convex curves, we are also interested in BÉZIER curves that have a single inflection point within the parameterization of  $[0, 1]$ . This includes curves with one overall inflection point (see Figure 7a) or BÉZIER curves that have two inflection points, of which only one is parameterized in  $[0, 1]$  (see Figure 7b). Precisely, in Figure 7b,  $I_1$  lies within the convex hull defined by the points  $P_0, P_1, P_2$  and  $P_3$  (parameterized on  $[0, 1]$ ), whereas  $I_2$  lies outside this convex hull. The numerical values defining the curves on Figure 7 are given on Table 1.

Throughout this article, we will refer to a curve with only one inflection point within the interval  $[0, 1]$  as mono-inflective. In Figure 7, inflection points are indicated by a round graphic bullet on a white background, labeled by the letter "I" and indexed as needed.

Additionally, we provide an example of a BÉZIER curve that contains two inflection points within the interval  $[0, 1]$  to clarify the concept of a mono-inflective curve in this range and to derive the necessary condition for this scenario.

To differentiate between the cases presented in Figure 7a and Figure 7b, we analyze the determinants of  $B^I(t)$  and  $B^{II}(t)$ . Given that  $B(t) = (X(t), Y(t))$ , we define  $\Gamma(t) = \det(B^I(t), B^{II}(t))$ , which corresponds to the expression in Formula (2).

$$\Gamma(t) = X^I(t) Y^{II}(t) - X^{II}(t) Y^I(t) \tag{2}$$

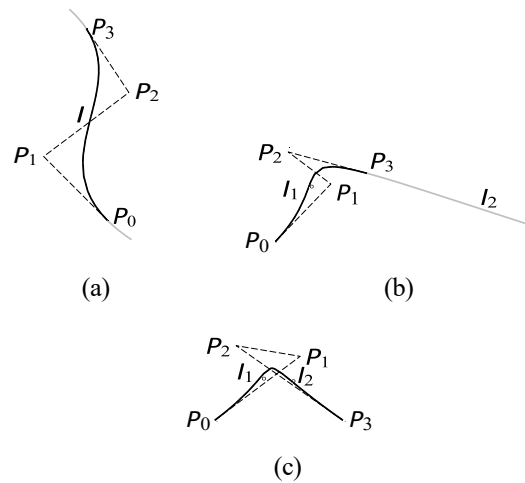


Figure 7: Inflective cubic Bézier curves: a single global inflection point (a), two inflection Points, one inside and one outside  $[0, 1]$  (b) and two inflection points inside  $[0, 1]$  (c)

Upon finalizing the calculations, we find that the function  $\Gamma$  is typically of degree at most two. The value  $\Gamma(t)$  can be expressed in the form given by Formula (3).

$$\Gamma(t) = A_2t^2 + A_1t + A_0 \tag{3}$$

Solutions to the equation  $\Gamma(t) = 0$  indicate the presence of inflection points. The discriminant  $\Delta$  on Formula (4) becomes an important quantity. In [22, 24], it is shown that:

$$\Delta = A_1^2 - 4A_2A_0 \tag{4}$$

- If  $A_2 = 0$ , then  $\Gamma(t)$  is of degree 1 and has a single solution, resulting in only one inflection point.
- If  $\Delta > 0$ , there are exactly two inflection points.
- If  $\Delta < 0$ , a node is present.
- If  $\Delta = 0$ , a cusp is formed.

In the first case of curves, as illustrated in Figure 7, the degree is one, which means there is only one solution. Consequently, the curve has a single inflection point.

In the other two curve cases,  $\Gamma(t)$  is a trinomial that allows for two solutions. For the second curve, the curvature vanishes at one point within the interval  $[0, 1]$  and at another point outside this interval. As a result, one inflection point lies inside the convex hull, while the other lies outside.

In the final curve case, both solutions are located within the interval  $[0, 1]$ , so both inflection points are contained within the convex hull.

A summary of the processing details for curves  $B_a$ ,  $B_b$  and  $B_c$ , relatively to Figure 7, is provided in Tables 1 and 2 for verification.

Table 2: Processing details: parameters and inflection points

Curve	Parameters and Inflection Points	
$B_a$	$t \simeq .5384$	–
	$l = (2.1302, 58.4615)$	–
$B_b$	$t_1 \simeq .3856$	$t_2 \simeq 1.315$
	$l_1 = (65.4634, 163.136)$	$l_2 = (148.164, 152.698)$
$B_c$	$t_1 \simeq .3009$	$t_2 \simeq .7616$
	$l_1 = (41.1811, 49.8819)$	$l_2 = (55.8477, 48.4152)$

We have previously mentioned that the types of curves relevant to this research are convex and mono-inflective ones, which are parameterized on the interval  $[0, 1]$ . Based on the figures of the curves we've examined so far, we can identify two important properties—perceived graphically—that characterize cubic BÉZIER curves.

Consider the BÉZIER curve  $B = [P_0, P_1, P_2, P_3]$ . We have the following observations:

1. If the line segments  $[P_0, P_1]$  and  $[P_2, P_3]$  intersect i.e.,  $[P_0, P_1] \cap [P_2, P_3] \neq \emptyset$ , then the curve  $B$  has either two inflection points, a cusp, or forms a loop.
2. If the line segments  $[P_0, P_1]$  and  $[P_2, P_3]$  do not intersect i.e.,  $[P_0, P_1] \cap [P_2, P_3] = \emptyset$ , this is a necessary condition for the curve  $B$  to be an arch (whether convex or not) or to be mono-inflective.

As for a convex BÉZIER curve, we have an accurate way to check if a BÉZIER curve is mono-inflective. Let  $B = [P_0, P_1, P_2, P_3]$  be a cubic BÉZIER curve where  $[P_0, P_1]$  and  $[P_2, P_3]$  do not intersect. The vectors  $U, V$  and  $T$  are such that  $B = [P_0, P_0 + U, P_0 + T - V, P_0 + T]$ . The curve  $B$  is mono-inflective if  $(P_1 - P_0) \times (P_2 - P_1)$  and  $(P_2 - P_1) \times (P_3 - P_2)$  are of opposite sign. The same thing is expressed as:  $U \times (T - V)$  and  $(T - U) \times V$  are opposite in terms of the sign.

We introduce a few notations to facilitate mathematical expression and formalization.

Let  $U_1$  and  $U_2$  be two vectors in  $\mathbb{R}^2$ . We denote  $U_1 \parallel U_2$  to indicate that  $U_1$  and  $U_2$  are collinear and point in the same direction.

When  $n$  vectors  $U_1, \dots, U_n$  are linearly independent, we refer to them as "free" vectors; conversely, if they are linearly dependent, we call them "linked" vectors. In this case, the set  $\{U_1, \dots, U_n\}$  is said to be free or linked, depending on the context.

## OBLIQUE CUBIC BÉZIER CURVES

### Obliquity: definitions, types and properties

We define a BÉZIER curve  $B(t) = (X(t), Y(t))$  in  $\mathbb{R}^2$  as oblique if the functions  $X(t)$  and  $Y(t)$  are strictly monotone on the interval  $[0, 1]$ .

We say that an oblique BÉZIER curve  $B$  is of type  $T_i$ , for  $1 \leq i \leq 4$ , if its base vector  $T = B(1) - B(0)$  is in quadrant  $Q_i$ . We can visually observe that the base vector  $T$  of an oblique cubic BÉZIER curve is necessarily located in a quadrant. This means that vector  $T$  can never be strictly horizontal or vertical. The study conducted in this section on oblique curves will, without loss of generality, take place in the first quadrant  $Q_1$ . We present some useful lemmas and a theorem that will aid in developing the interpolation method.

**Lemma 1.** Let  $B = [P_1, P_1 + U_1, P_2 - U_2, P_2]$  a cubic Bézier curve and  $\{U_1, U_2\}$  a set (not necessarily free) of non-null vectors. Consider  $T = P_2 - P_1$  such that  $T$  is in  $Q_1$  ( $T$  is oblique). Assume that  $\{U_1, T\}$  and  $\{U_2, T\}$  are free sets and the vectors  $U_1$  and  $U_2$  satisfy the condition:  $U_1, U_2 \in \mathbb{R}_T^-$  or  $U_1, U_2 \in \mathbb{R}_T^+$ . Then  $B$  is oblique.

*Proof.*

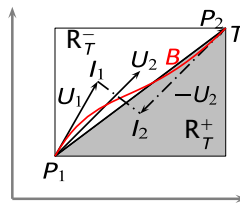


Figure 8: Lemma 1 conditions on  $Q_1$  quadrant

Assume that  $U_1 \in \mathbb{R}_T^-$  and  $U_2 \in \mathbb{R}_T^-$ . The proof remains the same if both  $U_1$  and  $U_2$  are in  $\mathbb{R}_T^+$ . Then  $U_1 = (r_1\sigma_1T_x, r_1T_y)$  and  $U_2 = (r_2\sigma_2T_x, r_2T_y)$  where  $0 \leq \sigma_1, \sigma_2 \leq 1$  and  $0 < r_1, r_2 \leq 1$ . Let us prove that  $B$  is oblique.

Consider that  $B(t) = (X(t), Y(t))$  for  $t \in [0, 1]$ .

Let us demonstrate that  $X'(t)$  and  $Y'(t)$  do not change in sign on  $[0, 1]$  and so  $X(t)$  and  $Y(t)$  are monotonic. All calculations done, we have:

$$\begin{aligned}
 X'(t) &= T_x (9r_1\sigma_1 - 6 + 9r_2\sigma_2)t^2 + \\
 &\quad (-12r_1\sigma_1 + 6 - 6r_2\sigma_2)t + \\
 &\quad 3r_1\sigma_1
 \end{aligned} \tag{5}$$

$$\begin{aligned}
 Y'(t) &= T_y (9r_1 - 6 + 9r_2)t^2 + \\
 &\quad (-12r_1 + 6 - 6r_2)t + \\
 &\quad 3r_1
 \end{aligned} \tag{6}$$

To study the signs of  $\mathcal{X}(t)$  and  $\mathcal{Y}(t)$ , it suffices to examine the signs of the functions  $F$  and  $G$  defined in (7) and (8).

$$F(t) = \frac{(9r_1\sigma_1 - 6 + 9r_2\sigma_2)t^2 + (-12r_1\sigma_1 + 6 - 6r_2\sigma_2)t + 3r_1\sigma_1}{3r_1\sigma_1} \quad (7)$$

$$G(t) = \frac{(9r_1 - 6 + 9r_2)t^2 + (-12r_1 + 6 - 6r_2)t + 3r_1}{3r_1} \quad (8)$$

We will begin by examining the sign of  $G(t)$ , which will help us deduce the sign of  $F(t)$ . The analysis of the sign of  $G(t)$  depends on two variables,  $r_1$  and  $r_2$ , and is not straightforward to carry out directly. Instead, we will approach this by studying  $G'(t)$ . The expression for  $G'(t)$  can be found on Formula (9).

$$G'(t) = 6((3r_1 + 3r_2 - 2)t - 2r_1 - r_2 + 1) \quad (9)$$

$G'(t)$  is an affine function and therefore has a single root,  $t_y$ , which is found in Formula (10):

$$t_y = \frac{2r_1 + r_2 - 1}{3r_1 + 3r_2 - 2} \quad (10)$$

We aim to study the sign of  $\mathcal{Y}$  on  $[0, 1]$ . To do this, we need to analyze the cases where  $t_y$  belongs to  $[0, 1]$ .

The value of  $t_y$ , which is a function of  $r_1$  and  $r_2$ , highlights two straight lines, which are subsets of  $\mathbb{R}^2$ . These lines are denoted  $(D_1)$  and  $(D_2)$  as described in Formulas (11) and (12).

$$(D_1) : 2r_1 + r_2 - 1 = 0 \quad (11)$$

$$(D_2) : 3r_1 + 3r_2 - 2 = 0 \quad (12)$$

To the straight lines  $(D_1)$  and  $(D_2)$ , correspond the functions  $D_1$  and  $D_2$  such that:

$$D_1 : \begin{matrix} \mathbb{R}^2 & \longrightarrow & \mathbb{R} \\ (r_1, r_2) & \longrightarrow & 2r_1 + r_2 - 1 \end{matrix} \quad (13)$$

$$D_2 : \begin{matrix} \mathbb{R}^2 & \longrightarrow & \mathbb{R} \\ (r_1, r_2) & \longrightarrow & 3r_1 + 3r_2 - 2 \end{matrix} \quad (14)$$

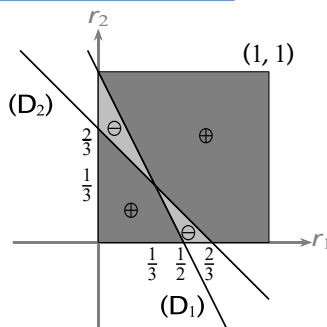


Figure 9: Sign areas of  $t_y$  as a function of  $r_1$  and  $r_2$

The fact that  $r_1, r_2 \in [0, 1]$  and considering the straight lines in  $\mathbb{R}^2$ ,  $(D_1)$  and  $(D_2)$ , in Figure 9, the ranges of  $(r_1, r_2)$  for which  $t_y > 0$  and  $t_y < 0$  are shown. We must remember that  $t_y = \frac{D_1(r_1, r_2)}{D_2(r_1, r_2)}$ . There are three cases to consider:

**Case 1 :**  $t_y < 0$ .

This case is feasible, we proceed with the following:  
 $(r_1, r_2) = (7/12, 1/24), D_1(7/12, 1/24) = \frac{5}{24}, D_2(7/12, 1/24) = -\frac{1}{8}, t_{y,(7/12,1/24)} = -\frac{5}{3}$ .  
 or  
 $(r_1, r_2) = (1/12, 7/9), D_1(1/12, 7/9) = -\frac{1}{18}, D_2(1/12, 7/9) = \frac{7}{12}, t_{y,(1/12,7/9)} = -\frac{2}{21}$ .

In this case,  $G'(t)$  doesn't change sign on  $[0, 1]$ .

Thus,  $G$  is strictly monotone on  $[0, 1]$ .

Given that  $G(0) = 3r_1 > 0$  and  $G(1) = 3r_2 > 0$ , we have  $G(t) > \min(3r_1, 3r_2) > 0 \forall t \in [0, 1]$ .

Therefore,  $Y'(t) > 0, \forall t \in [0, 1]$ .

Consequently,  $Y(t)$  is strictly increasing on  $[0, 1]$ .

**Case 2 :**  $t_y > 1$ .

This case is feasible, we proceed with the following:  
 $(r_1, r_2) = (5/6, 1/24), D_1(5/6, 1/24) = \frac{17}{24}, D_2(5/6, 1/24) = \frac{5}{8}, t_{y,(5/6,1/24)} = \frac{17}{15}$ .  
 or  
 $(r_1, r_2) = (1/12, 1/2), D_1(1/12, 1/2) = -\frac{1}{3}, D_2(1/12, 1/2) = -\frac{1}{4}, t_{y,(1/12,1/2)} = \frac{4}{3}$ .

The same reasoning as before is applied to conclude that  $Y(t)$  is strictly increasing on  $[0, 1]$ .

**Cas 3 :**  $0 \leq t_y \leq 1$ .

This case is well feasible, we take the following for examples:  
 $(r_1, r_2) = (2/3, 1/2), D_1(2/3, 1/2) = \frac{5}{6}, D_2(2/3, 1/2) = \frac{3}{2}, t_{y,(2/3,1/2)} = \frac{5}{9}$ .

Or  
 $(r_1, r_2) = (1/3, 1/6), D_1(1/3, 1/6) = -\frac{1}{6}, D_2(1/3, 1/6) = -\frac{1}{2}, t_{y,(1/3,1/6)} = \frac{1}{3}$ .

Let us prove that  $Y(t)$  is strictly increasing. We recall that the sign of the function  $G$  is the same as that of  $Y'$ . We have:

$$G(0) = 3r_1 > 0 \forall r_1 \in ]0, 1] \text{ and}$$

$$G(1) = 3r_2 > 0 \quad \forall r_2 \in ]0, 1].$$

If we can demonstrate that  $G(t_y) \geq 0$ , then  $G$  does not change sign on  $[0, 1]$ , which implies that  $Y(t)$  is strictly increasing on  $[0, 1]$ .

The value of  $G(t_y)$  is a function of  $r_1$  and  $r_2$  as outlined in Formula (15).

$$G(t_y) = -3 \frac{r_1^2 - 2r_1 + r_1 r_2 - 2r_2 + r_2^2 + 1}{3r_1 + 3r_2 - 2} \quad (15)$$

Let us study  $G(t_y)$  as a function of  $r_1$  and  $r_2$  on  $[0, 1]^2$ .

We have,  $0 \leq t_y \leq 1$ :

$$G'(t_y) = 0 \quad (16)$$

$$G'(0) = -12r_1 - 6r_2 + 6 \quad (17)$$

$$G'(1) = 6r_1 + 12r_2 - 6 \quad (18)$$

We recall that  $G'(t)$  is affine and, so there are two cases that fall under **Case 3**:

$$1. \quad G'(0) < 0 \text{ and } G'(1) > 0$$

$$2. \quad G'(0) > 0 \text{ and } G'(1) < 0$$

To begin analysing the sign of  $G(t_y)$ , we define two functions  $f_y$  and  $g_y$ , as shown in Formulas (19) and (20).

$$f_y : \mathbb{R}^2 \rightarrow \mathbb{R} \\ (r_1, r_2) \rightarrow r_1^2 - 2r_1 + r_1 r_2 - 2r_2 + r_2^2 + 1 \quad (19)$$

$$g_y : \mathbb{R}^2 \rightarrow \mathbb{R} \\ (r_1, r_2) \rightarrow 3r_1 + 3r_2 - 2 \quad (20)$$

$$\text{We have then } G(t_y) = -3 \frac{f_y(r_1, r_2)}{g_y(r_1, r_2)}.$$

**Case 3-1** :  $G'(0) < 0$  and  $G'(1) > 0$

In this case  $t_y$  represents a minimum of  $G$ .

Analysing the sign of  $f_y$  on  $[0, 1]^2$  is challenging without delving into optimization concepts.

Let us study the extrema of  $f_y$  on  $[0, 1]^2$ .

The signs of  $G'(0)$  and  $G'(1)$  highlight two functions  $D_3$  and  $D_4$  defined in Formulas (21) and (22) as well as the two affine lines  $(D_3)$  and  $(D_4)$  defined in (23) and (24).

$$D_3 : \mathbb{R}^2 \rightarrow \mathbb{R} \\ (r_1, r_2) \rightarrow -12r_1 - 6r_2 + 6 \quad (21)$$

$$D_4 : \mathbb{R}^2 \rightarrow \mathbb{R} \\ (r_1, r_2) \rightarrow 6r_1 + 12r_2 - 6 \quad (22)$$

$$(D_3) : -2r_1 - r_2 + 1 = 0 \tag{23}$$

$$(D_4) : r_1 + 2r_2 - 1 = 0 \tag{24}$$

$G^l(0) < 0$ , i.e.  $D_3(r_1, r_2) < 0$ , provides the constraint denoted  $(C_1)$ :

$$(C_1) : -2r_1 - r_2 + 1 < 0 \tag{25}$$

$G^l(1) > 0$ , i.e.  $D_4(r_1, r_2) > 0$ , provides the constraint denoted  $(C_2)$ :

$$(C_2) : -r_1 - 2r_2 + 1 < 0 \tag{26}$$

Let us study the extrema of  $f_y$  under the constraints  $(C_1)$  and  $(C_2)$ .

The variables  $r_1$  and  $r_2$  must adhere to the constraints  $(C_3)$ ,  $(C_4)$ ,  $(C_5)$  and  $(C_6)$  specified on Formulas (27)–(30).

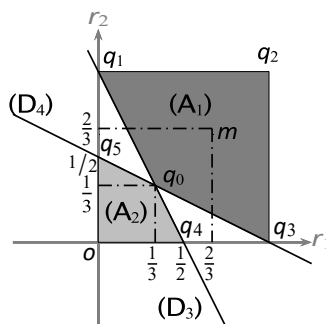


Figure 10: Optimization areas relative to different signs of  $G^l$  on 0 and 1

$$(C_3) : r_1 - 1 \leq 0 \tag{27}$$

$$(C_4) : -r_1 \leq 0 \tag{28}$$

$$(C_5) : r_2 - 1 \leq 0 \tag{29}$$

$$(C_6) : -r_2 \leq 0 \tag{30}$$

The constraints  $(C_1)$ ,  $(C_2)$ ,  $(C_3)$ ,  $(C_4)$ ,  $(C_5)$  and  $(C_6)$  enable us to draw the graphic on Figure 10.

$$(A_1) : (r_1, r_2) \in \mathbb{R}^2 / (r_1, r_2) \in \bigcap_{i=1}^6 (C_i) \tag{31}$$

The subset of  $[0, 1]^2$  where  $G^l(0) < 0$  and  $G^l(1) > 0$  is defined as the set  $(A_1)$  in Formula (31).

The set  $(A_1)$  is the gray area shown in Figure 10. This is the compact of segment-shaped edges bounded by points  $q_0$ ,  $q_1$ ,  $q_2$  and  $q_3$ .

Let's find the minimum of  $f_y$  on  $(A_1)$ .

The set  $(A_1)$  is closed and bounded.

So, according to WEIRstRass,  $f_y$  has a minimum on  $(A_1)$ .

The gradient of  $f_y$  is :

$$\nabla_f (r_1, r_2) = \begin{pmatrix} 2r_1 + r_2 - 2 \\ r_1 + 2r_2 - 2 \end{pmatrix} .$$

The function  $f_y$  has only one critical point, which is located at  $m = (2/3, 2/3)$ . This critical point is contained within  $(A_1)$ .

Let  $H_y$  be the hessian matrix relative to  $f_y$ .

$$\text{We have } H_y = \begin{pmatrix} 2 & 1 \\ 1 & 2 \end{pmatrix}$$

The matrix  $H_y$  is positive-definite. So,  $f_y$  is strictly convex on  $(A_1)$ .

Hence  $m = (2/3, 2/3)$  is the unique minimum relative to  $f_y$  on  $(A_1)$ .

We have  $f_y(2/3, 2/3) = -1/3 < 0$ .

Notice that the objective is to determine the sign of  $f_y$  on  $(A_1)$ .

Let us study the sign of  $f_y$  on the boundary of  $(A_1)$ .

$/r(S)$  : denotes the boundary of a given set  $S$ .

Let  $(r_1, r_2) \in /r(A_1)$ ,  $(r_1, r_2)$  is in one of the four following cases :

- $(r_1, r_2) \in [q_0, q_3]$ ,  $r_1 = 1 - 2r_2$ , let  $q \in [q_0, q_3]$ , then  $q = (1 - 2r_2, r_2)$   
 $f_y(q) = f_y(1 - 2r_2, r_2) = r_2(3r_2 - 1)$   
 We have  $f_y(q) \leq 0$  since  $(r_1, r_2) \in [q_0, q_3]$  and so  $0 \leq r_2 \leq 1/3$ .
- $(r_1, r_2) \in [q_0, q_1]$ ,  $r_2 = 1 - 2r_1$ , let  $q \in [q_0, q_1]$ , then  $q = (r_1, 1 - 2r_1)$   
 $f_y(q) = f_y(r_1, 1 - 2r_1) = r_1(3r_1 - 1)$   
 We get that  $f_y(q) \leq 0$  since  $(r_1, r_2) \in [q_0, q_1]$  and so  $0 \leq r_1 \leq 1/3$ .
- $(r_1, r_2) \in [q_1, q_2]$ ,  $r_2 = 1$ , let  $q \in [q_1, q_2]$ , then  $q = (r_1, 1)$   
 $f_y(q) = f_y(r_1, 1) = r_1(r_1 - 1)$   
 We have  $f_y(q) \leq 0$  due to the fact that if  $(r_1, r_2) \in [q_1, q_2]$  then  $0 \leq r_1 \leq 1$ .
- $(r_1, r_2) \in [q_2, q_3]$ ,  $r_1 = 1$ , let  $q \in [q_2, q_3]$ , so  $q = (1, r_2)$   
 $f_y(q) = f_y(1, r_2) = r_2(r_2 - 1)$   
 We get  $f_y(q) \leq 0$  due to the fact that if  $(r_1, r_2) \in [q_2, q_3]$  then  $0 \leq r_2 \leq 1$ .

We observe that  $f_y$  is *negative* on the boundary of  $(A_1)$  and has a minimum  $m$  strictly interior to  $(A_1)$  where  $f_y(m) < 0$ . So,  $f_y$  is negative on  $(A_1)$  as a whole, otherwise we'll lose out in terms of convexity.

Hence:

$$f_y(r_1, r_2) \leq 0 \quad \forall (r_1, r_2) \in A_1$$

Now let's look at the sign of  $g_y$ .

Let  $(r_1, r_2) \in (A_1)$

Then  $(r_1, r_2)$  satisfies  $(C_1)$  and  $(C_2)$ .

$$\begin{aligned} (C_1) + (C_2) & \Rightarrow -3r_1 - 3r_2 + 2 \leq 0 \\ & \Rightarrow g_y(r_1, r_2) \geq 0 \end{aligned}$$

So, on  $(A_1)$ , with  $g_y(r_1, r_2) \neq 0$ , we get that  $g_y(r_1, r_2) > 0$

We then deduce that  $-3 \frac{f_y(r_1, r_2)}{g_y(r_1, r_2)} \geq 0$  on  $[0, 1]^2$ .

Thus, we get that  $G(t_y) \geq 0$  over  $[0, 1]^2$

Given that  $t_y$  is a minimum of  $G$  on  $[0, 1]$ , then  $G(t) \geq 0, \forall t \in [0, 1]$ .

So,  $Y'(t) \geq 0, \forall t \in [0, 1]$ .

Therefore,  $Y(t)$  is increasing on  $[0, 1]$ .

With the feasible values of  $r_1$  and  $r_2$  meeting the constraints of inscription in the affine rectangle and considering the cases where vectors  $U_1, U_2$  and  $T$  are not null, we can conclude that  $Y(t)$  is strictly increasing on  $[0, 1]$ .

**Case 3-2 :**  $G'(0) > 0$  and  $G'(1) < 0$

The subset of  $[0, 1]^2$  where  $G'(0) > 0$  and  $G'(1) < 0$  is defined as the set  $(A_2)$  shown in Figure (10). In this case, at  $t_y$  there is a maximum of  $G$  on  $[0, 1]$ .

We have :

$$G(0) = 3r_1 > 0 \quad \forall r_1 \in ]0, 1]$$

$$G(1) = 3r_2 > 0 \quad \forall r_2 \in ]0, 1]$$

So,  $G(t_y) \geq 0 \quad \forall t \in [0, 1]$

Due to the uniqueness of the optimum  $t_y$  on  $[0, 1]$  We get that  $G(t) \geq 0 \quad \forall t \in [0, 1]$ .

It follows that  $Y'(t) \geq 0 \quad \forall t \in [0, 1]$

So  $Y(t)$  is increasing on  $[0, 1]$ .

With the feasible values of  $r_1$  and  $r_2$  meeting the constraints of inscription in the affine rectangle and considering the cases where vectors  $U_1, U_2$  and  $T$  are not null, we can conclude that  $Y(t)$  is strictly increasing on  $[0, 1]$ .

Now it's time to show that  $X(t)$  is also strictly increasing on  $[0, 1]$ .

To analyze the sign of  $X'(t)$ , we need only to study that of  $F(t)$  defined in (7).

We'll use the function  $G(t)$  (having the same sign as  $Y'(t)$ ), given in (8), to deduce that of  $F(t)$ . For ease of reference, let's rewrite the  $G$  function and the results we've found:

$$G(t) = (9r_1 - 6 + 9r_2)t^2 + (-12r_1 + 6 - 6r_2)t + 3r_1$$

We proved before the following result:

$$\forall (r_1, r_2) \in [0, 1]^2, G(t) \geq 0, \forall t \in [0, 1] \tag{32}$$

Function  $F$  is written as:

$$F(t) = (9r_1\sigma_1 - 6 + 9r_2\sigma_2)t^2 + (-12r_1\sigma_1 + 6 - 6r_2\sigma_2)t + 3r_1\sigma_1$$

$r_1, r_2, \sigma_1, \sigma_2 \in [0, 1]^4$  et  $t \in \mathbb{R}$

Let  $y_1 = r_1\sigma_1$  and  $y_2 = r_2\sigma_2$ .

Then we have  $y_1 \in [0, 1]$  and  $y_2 \in [0, 1]$ .

The formula of  $F(t)$  becomes :

$$F(t) = (9y_1 - 6 + 9y_2)t^2 + (-12y_1 + 6 - 6y_2)t + 3y_1$$

According to (32), we have:

$$\forall (y_1, y_2) \in [0, 1]^2, F(t) \geq 0, \forall t \in [0, 1].$$

Finally, we get the result on (33):

$$\forall (r_1, r_2, \sigma_1, \sigma_2) \in [0, 1]^4, F(t) \geq 0, \forall t \in [0, 1] \quad (33)$$

From this, we get that  $X'(t) \geq 0$  on  $[0, 1]$  and thus  $X(t)$  is increasing on  $[0, 1]$ .

With the possible cases of  $r_1, r_2, \sigma_1$  and  $\sigma_2$  meeting the constraints of inscription in the vector rectangle and considering the cases where vectors  $U_1, U_2$  and  $T$  are not null,  $X(t)$  is strictly increasing on  $[0, 1]$ .

We conclude that the BÉZIER curve  $B$  is *oblique*. □

We deal now with the case where the vector  $U_1$  and  $U_2$  participating in the definition of the BÉZIER curve are in opposite sign in belonging to  $R_T$ .

**Lemma 2.** *Let  $B = [P_1, P_1 + U_1, P_2 - U_2, P_2]$  a cubic Bézier curve. Consider  $T = P_2 - P_1$  such that  $T$  is in  $Q_1$  ( $T$  is strongly oblique). Assume that  $\{U_1, T\}$  and  $\{U_2, T\}$  are free sets. Vectors  $U_1$  and  $U_2$  meet the condition:  $U_1 \in R_T^-$  and  $U_2 \in R_T^+$  or  $U_1 \in R_T^+$  and  $U_2 \in R_T^-$ . Then  $B$  is oblique.*

*Proof.*

Assume that  $U_1 \in R_T^-$  and  $U_2 \in R_T^+$  (the proof remains the same when  $U_1 \in R_T^+$  and  $U_2 \in R_T^-$ ).

The change, comparing to the proof done before, would happen in  $U_2$  parameterizing.

Let  $U_1 = (r_1\sigma_1 T_x, r_1 T_y)$  and  $U_2 = (r_2 T_x, r_2\sigma_2 T_y)$  where  $0 \leq \sigma_1, \sigma_2 \leq 1$  and  $0 < r_1, r_2 \leq 1$

Given that  $B(t) = (X(t), Y(t))$  for  $t \in [0, 1]$ , all calculations done,  $X'(t)/T_x$  and  $Y'(t)/T_y$  are on Formula (34) and (35)

$$\begin{aligned} X'(t)/T_x &= \frac{(9r_1\sigma_1 - 6 + 9r_2)t^2 + (-12r_1\sigma_1 + 6 - 6r_2)t + 3r_1\sigma_1}{3r_1\sigma_1} \end{aligned} \quad (34)$$

$$\begin{aligned} Y'(t)/T_y &= \frac{(9r_1 - 6 + 9r_2\sigma_2)t^2 + (-12r_1 + 6 - 6r_2\sigma_2)t + 3r_1}{3r_1} \end{aligned} \quad (35)$$

Let  $\mu_1 = r_1\sigma_1$ , then  $\mu_1$  describe the interval  $[0, 1]$ .

Replacing  $r_1\sigma_1$  with  $\mu_1$ , Formula (34) becomes like (8).

So,  $X(t)$  is strictly increasing on  $[0, 1]$ .

Following the same method, we get that  $Y(t)$  is strictly increasing on  $[0, 1]$ .

We conclude that  $B$  is oblique. □

The aforementioned cases concerning the positions of  $U_1$  and  $U_2$  in  $R_T$  and their relationship with the vector  $T$  are not the only ones. In fact, other situations exist such as when  $U_1 \perp T, U_2 \perp T$  or  $U_1 \perp U_2 \perp T$ . However, the sequences considered in this paper concern the non-degenerate cases. In such cases, and as

we'll see, we won't have the degenerate position cases;  $U_1 \parallel T, U_2 \parallel T$  or  $U_1 \parallel U_2 \parallel T$ , because of the way we use to construct directions at points in the sequence.

The lemmas seen before, Lemma 1 and Lemma 2, are bases to state and prove the following theorem.

**Theorem 1.** Consider  $U_1, U_2$  and  $T$  three non null vectors in  $\mathbb{R}^2$  such that  $T \in Q_1$  and  $U_1, U_2 \in R_T$ . Let  $B = [P_1, P_1 + U_1, P_2 - U_2, P_2]$  where  $P_2 - P_1 = T$ . Assume that  $\{U_1, T\}$  and  $\{U_2, T\}$  are free sets. Then  $B$  is oblique.

It is interesting to cite all the possible cases of the oblique cubic BÉZIER curves defined based on the state of vector's belonging to vector rectangle. The idea is presented with using figures and discussing cases for more clarification.

1.  $U_1, U_2 \in R_T^-$  or  $U_1, U_2 \in R_T^+$

This case is illustrated on Figure 8 considering that  $U_1, U_2 \in R_T^-$ . The curve is oblique with one inflection point. In fact, in this case the arms  $[P_0, I_1]$  and  $[P_2, I_2]$  don't intersect and  $U_1 \times (T - U_2)$  and  $(T - U_1) \times U_2$  are of opposite sign.

2.  $U_1 \in R_T^I$  and  $U_2 \in R_T^I$  or  $U_1 \in R_T^I$  and  $U_2 \in R_T^I$

The case is illustrated on Figures 11–13 with  $U_1 \in R_T^-$  and  $U_2 \in R_T^+$ . A curve satisfying this constraint is oblique and can be convex (see Figure 11), mono-inflective (see Figure 12) or can have two inflection points (see Figure 13).

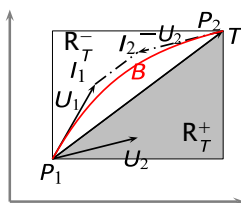


Figure 11: Lemma 2 conditions - Oblique convex Curve

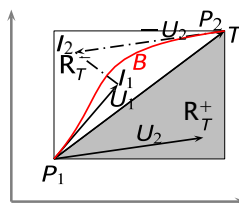


Figure 12: Lemma 2 conditions - Oblique mono-Inflective Curve

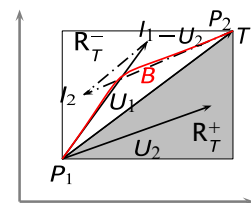


Figure 13: Lemma 2 conditions - Oblique Curve with two inflection points

### Convex oblique curves

An oblique BÉZIER curve  $B = [P_1, P_1 + U_1, P_2 - U_2, P_2]$  of type  $T_i$  that is also convex can be further classified into sub-types  $T_i^+$  and  $T_i^-$  depending on the sign of  $U_1 \times T$ , where  $T = P_2 - P_1$ ; that is, whether the initial velocity vector  $B'(0) = 3U_1$  lies clockwise or counterclockwise of the base vector  $T$  (see Figure 14).

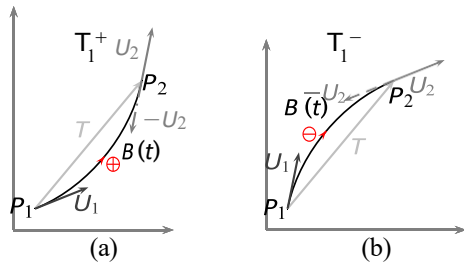


Figure 14: Examples of convex oblique curves of sub-types  $T_1^+$  (left) and  $T_1^-$  (right)

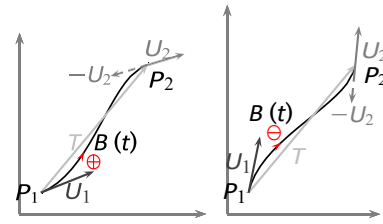


Figure 15: Examples of Mono-inflective oblique curves of sub-types  $T_1^+$  (left) and  $T_1^-$  (right)

Let us consider a BÉZIER curve  $B = [P_1, P_1 + U_1, P_2 - U_2, P_2]$  where  $P_2 - P_1 = T$ ,  $T \in Q_1$  and  $U_1, U_2 \in R_T$ . From Lemma 2, we learn that the only case where  $B$  can be oblique convex is the fact that the belonging signs of vectors  $U_1$  and  $U_2$  to  $R_T$  are opposite. This is a necessary condition.

### Mono-inflective oblique curves

The aim of our work is to develop a method allowing interpolation of oblique sequences of points in the plane with keeping convexity and inflection properties. The oblique curves we are interested to are convex and mono-inflective ones. By referring to Lemma 1 and Lemma 2, we find that the mono-inflective, in the non-degenerate case, are of two types depending on whether  $U_1$  and  $U_2$ , with a curve  $B = [P_1, P_1 + U_1, P_1 + T - U_2, P_1 + T]$ , have the same or opposite sign in belonging to  $R_T$ . Lemma 1 highlights mono-inflective curves that cross the base  $T$ , whereas Lemma 2 reveals ones not crossing the base of the curve. We retain the first type as one of the basic curves in interpolation method since this type aids in keeping as possible the topology of the sequence of points.

Like the case of oblique convex BÉZIER curves, oblique mono-inflective ones (satisfying Lemma 1 of course) are of four signed types. Given an oblique BÉZIER curve  $B = [P_1, P_1 + U_1, P_1 + T - U_2, P_1 + T]$ , then the sign of  $B$  is relative to the position of the vector  $U_1$  with respect to vector  $T$ , as in the case of oblique convex curves, i.e. the sign of  $U_1 \times T$ . The sign is not quite the direction of the turning sens in the orthonormal reference, as in the case of convex oblique curves, since this direction changes once the inflection point is crossed. However, it's still the direction in which the curve turns from  $P_1$  to the inflection point. An illustration is given in Figure 15.

A basic lemma for building mono-inflective BÉZIER curves from vectors with opposite signs in terms of belonging to the vector rectangle is stated (see Lemma 3). The lemma is essential to the interpolation process.

**Lemma 3.** *Let  $U_1, U_2$ , and  $T$  be three vectors in  $R^2$  two-by-two linearly independent. Assume that  $T$  is oblique,  $U_1 \in R_T$  and  $U_2 \in R_T$  where  $U_1$  and  $U_2$  have opposite sign of belonging to  $R_T$ . Consider the curve  $B$ ,  $P_1, P_2 \in R^2$  such that  $P_2 - P_1 = T$  and  $B = [P_1, P_1 + U_1, P_2 - \Omega_T(U_2), P_2]$ . The transform  $\Omega_T$  denotes the rectangular inversion relative to  $T$ . Then the curve  $B$  is mono-inflective oblique.*

*Proof.*

$U_1 \times T$  and  $T \times U_2$  are of opposite sign.

According to Property 2(2),  $\Omega_T(U_2)$  and  $U_2$  are of opposite sign in belonging to  $R_T$ .

So  $U_1$  and  $\Omega_T(U_2)$  belong to the same semi-vector rectangle of  $R_T$ .

Applying Lemma 1, we get that the curve  $B$  is mono-inflective oblique.

□

## OBLIQUE BÉZIER CURVES AND GENERATING SETS

In the previous sections, we saw that a curve can be expressed in a vector form. From this point of view, we notice that a cubic BÉZIER curve can be generated and studied on the basis of a set of three vectors and an origin point.

Given a set  $S = \{U_1, U_2, T\}$  of three non-null vectors, the BÉZIER curve  $B = [P_1, P_1 + \alpha_1 U_1, P_2 - \alpha_2 U_2, P_2]$ , such that  $P_2 = P_1 + T$  and  $\alpha_1, \alpha_2 \in \mathbb{R}^*$ , is said to be generated via  $S$ . The point  $P_1$  is called the origin of the curve. In the same time,  $P_1$  and  $P_2$  are named the extremities. The curve can be also written as  $B = [P_1, P_1 + \alpha_1 U_1, P_1 + T - \alpha_2 U_2, P_1 + T]$ . The notion of generating set that we have introduced can be applied to all cubic BÉZIER curves. In this paper, it will be used to study oblique BÉZIER curves, especially convex and mono-inflective ones. Here, the set  $S = \{U_1, U_2, T\}$  needs to meet some conditions, such as that the three vectors  $U_1, U_2$  and  $T$  must belong to the same closed quadrant, with  $T$  being oblique. Also, we have to notice that it is not mandatory that  $U_1 \in R_T$  nor  $U_2 \in R_T$ .

It should be clear that the study of oblique BÉZIER curves generated by a set  $S = \{U_1, U_2, T\}$  requires the distinction of different cases of relationship between the vectors  $U_1, U_2$  and  $T$ . This leads to two classes of cases: non-degenerate and degenerate states. We have to recall that the study of degenerate cases is out of the scope of this paper. In a first stage, we will state a lemma for constructing an oblique BÉZIER curve without any constraints on the type (convex, mono-inflective, two-inflective . . . ). The work is carried out with respect to the quadrant  $Q_1$ .

Let us consider the notations following:

$\bar{\mathbb{R}}$ : denote  $\mathbb{R} \cup \{-\infty, +\infty\} = [-\infty, +\infty]$ .

$\inf(a, b)$ : denotes the extended version of “inf” on  $\mathbb{R}$  and returns the smaller of  $a$  and  $b$  where  $a, b \in \bar{\mathbb{R}}$ .

**Lemma 4.** *Given a set of non-null vectors  $S = \{U_1, U_2, T\}$  in  $\mathbb{R}^2$  where  $U_1 \equiv U_{1,x}, U_{1,y}$ ,  $U_2 = U_{2,x}, U_{2,y}$  and  $T = (T_x, T_y)$ . Consider the quadrant  $Q_1$  such that  $T \in Q_1$  and  $U_1, U_2 \in Q_1$ . Let  $\alpha_1, \alpha_2 \in \mathbb{R}_+^*$ ,  $P_1, P_2 \in \mathbb{R}^2$  be such that  $P_2 = P_1 + T$  and  $B = [P_1, P_1 + \alpha_1 U_1, P_2 - \alpha_2 U_2, P_2]$  the curve generated by  $\{U_1, U_2, T\}$ . Suppose that  $\alpha_1$  and  $\alpha_2$  verify:  $\alpha_1 < \inf \frac{T_x}{U_{1,x}}, \frac{T_y}{U_{1,y}}$  and  $\alpha_2 < \inf \frac{T_x}{U_{2,x}}, \frac{T_y}{U_{2,y}}$ . Then  $B$  is oblique.*

*Proof.*

Let  $h_1 = \inf \frac{T_x}{U_{1,x}}, \frac{T_y}{U_{1,y}}$  and  $h_2 = \inf \frac{T_x}{U_{2,x}}, \frac{T_y}{U_{2,y}}$ .

For a vector  $V \in \mathbb{R}^2$ ,  $\hat{V}$  denotes the the angle between the X-axis and the vector  $V$  in the counterclockwise

sens.

We can check with comparing  $\tan \hat{V}$  and  $\tan \hat{T}$  that we have:

$$\inf_{V_x, V_y} \frac{T_x, T_y}{V_x, V_y} = \begin{cases} \frac{T_y}{V_y} & \text{if } V \times T \leq 0 \\ \frac{T_x}{V_x} & \text{otherwise} \end{cases}$$

With considering the possible values of  $h_1$  and  $h_2$ , we can deduce that  $h_1U_1$  and  $h_2U_2$  are two vectors with arrow heads exactly on the border of  $R_T$  (see Figure 16a and Figure 16b for illustration).

So,  $h_1U_1$  (resp  $h_2U_2$ ) is the vector positively colinear to  $U_1$  (resp  $U_2$ ) having the greater magnitude and inside  $R_T$ .

Thus, for  $\alpha_1, \alpha_2 \in \mathbb{R}^*$  such that  $\alpha_1 < h_1$  and  $\alpha_2 < h_2$ , we get that  $\alpha_1U_1 \in R_T$  and  $\alpha_2U_2 \in R_T$

According to Theorem 1,  $B$  is oblique

□

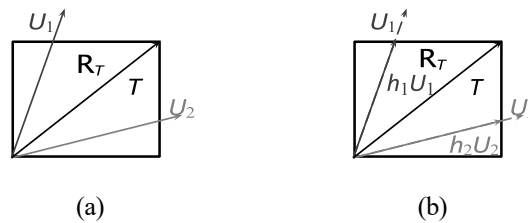


Figure 16: Generator vectors  $U_1$  and  $U_2$  (left), Generated vectors  $h_1U_1$  and  $h_2U_2$  with heads on the boundary of  $R_T$ .

To develop an interpolation method that maintains, when needed, convexity, inflections, and general topology, it's important to consider the most convenient types of oblique BÉZIER curves. These include curves that are convex and curves that are mono-inflective crossing their bases.

Consider curve  $B = [P_1, P_1 + \alpha_1U_1, P_2 - \alpha_2U_2, P_2]$ , generated by  $S = \{U_1, U_2, T\}$ . For curve  $B$  to be convex,  $U_1 \times T$  and  $T \times U_2$  must have the same sign. On the other hand,  $B$  can be mono-inflective crossing its base only if  $U_1 \times T$  and  $T \times U_2$  have opposite signs. These two cases are presented and discussed below.

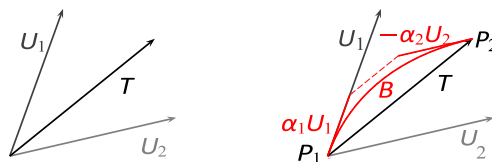


Figure 17: Example of non-degenerate convex oblique curve, generating set  $S = \{U_1, U_2, T\}$  (left) and generated curve (right)

**$U_1 \times T$  and  $T \times U_2$  in same sign**

**Lemma 5.** Given a set of non-null vectors  $S = \{U_1, U_2, T\}$  in  $\mathbb{R}^2$  such that  $\{U_1, T\}$  and  $\{U_2, T\}$  are free. Consider that  $T \in Q_1$  and  $U_1, U_2 \in Q_1$ . Assume that  $U_1 \times T$  and  $T \times U_2$  have the same sign. Let  $\alpha_1, \alpha_2 \in \mathbb{R}^*$ ,  $P_1, P_2 \in \mathbb{R}^2$  be such that  $P_2 = P_1 + T$  and  $B = [P_1, P_1 + \alpha_1 U_1, P_2 - \alpha_2 U_2, P_2]$  the curve generated by  $\{U_1, U_2, T\}$ . Suppose that  $\alpha_1$  and  $\alpha_2$  verify:  $\alpha_1 < \frac{T \times U_2}{U_1 \times U_2}$  and  $\alpha_2 < \frac{U_1 \times T}{U_1 \times U_2}$ . Then  $B$  is convex oblique.

*Proof.*

(see Figure 17 for illustration).

Let us first prove that  $B$  is oblique.

Let  $U_1 = U_{1,x} U_{1,y}$ ,  $U_2 = U_{2,x} U_{2,y}$  and  $T = T_x T_y$

Consider  $h_1 = \inf \frac{T_x}{U_{1,x}}, \frac{T_y}{U_{1,y}}$  and  $h_2 = \inf \frac{T_x}{U_{2,x}}, \frac{T_y}{U_{2,y}}$ .

Let us prove that  $\frac{T \times U_2}{U_1 \times U_2} \leq h_1$  and  $\frac{U_1 \times T}{U_1 \times U_2} \leq h_2$ .

Assume that  $U_1 \times T < 0$  and Then  $U_2 \times T > 0$  (This implies that  $U_{1,y} \neq 0$  and  $U_{2,x} \neq 0$ )

So  $h_1 = \frac{T_y}{U_{1,y}}$  and  $h_2 = \frac{T_x}{U_{2,x}}$ .

$$\begin{aligned} \frac{T \times U_2}{U_1 \times U_2} - h_1 &= \frac{T_x U_{2,y} - T_y U_{2,x}}{U_1 \times U_2} - \frac{T_y}{U_{1,y}} \\ &= \frac{T_x U_{2,y} - T_y U_{2,x}}{(U_1 \times U_2) U_{1,y}} \\ &= \frac{T_y U_{1,x} U_{2,y} - U_{1,y} U_{2,x}}{(U_1 \times U_2) U_{1,y}} \\ &= \frac{U_{2,y} T_x U_{1,y} - T_y U_{1,x}}{U_{1,y} (U_1 \times U_2)} \\ &= \frac{U_{2,y} (T \times U_1)}{U_{1,y} (U_1 \times U_2)} \end{aligned}$$

$U_1, U_2 \in Q_1$  implies that  $U_{1,y} \geq 0$  and  $U_{2,y} \geq 0$ .

Moreover,  $U_{1,y} > 0$  since  $T \times U_1 > 0$ .

We have that  $T \times U_1 > 0$  and  $U_1 \times U_2 < 0$ .

Thus  $\frac{T \times U_2}{U_1 \times U_2} - h_1 \leq 0$  and then  $\frac{T \times U_2}{U_1 \times U_2} \leq h_1$ .

After calculation, in the same way as before, we find that  $\frac{U_1 \times T}{U_1 \times U_2} - h_2 = \frac{U_{1,x} (U_2 \times T)}{U_{2,x} (U_1 \times U_2)} \leq 0$ .

Then  $\frac{U_1 \times T}{U_1 \times U_2} \leq h_2$ .

According to Lemma 4, for  $\alpha_1 < \frac{T \times U_2}{U_1 \times U_2}$  and  $\alpha_2 < \frac{U_1 \times T}{U_1 \times U_2}$ ,  $B$  is oblique.

Now we prove that the curve  $B$  is convex.

Since  $U_1, U_2$ , and  $T$  are in the same quadrant, and  $U_1 \times T$  and  $T \times U_2$  have the same sign  $\sigma$ , it follows that  $U_1 \times U_2$  also has that same sign  $\sigma$ .

From  $0 < \alpha_1$  and  $\alpha_1 < (T \times U_2) / (U_1 \times U_2)$  we get either  $\alpha_1 U_1 \times U_2 > 0$  and  $T \times U_2 - \alpha_1 U_1 \times U_2 > 0$ , or  $\alpha_1 U_1 \times U_2 < 0$  and  $T \times U_2 - \alpha_1 U_1 \times U_2 < 0$ , depending on  $\sigma$ .

Either way, it follows that  $T \times U_2 - \alpha_1 U_1 \times U_2 = (T - \alpha_1 U_1) \times U_2$  also has sign  $\sigma$ .

Similarly, from  $0 < \alpha_2$  and  $\alpha_2 < (U_1 \times T) / (U_1 \times U_2)$  we conclude that  $U_1 \times (T - \alpha_2 U_2)$  also has sign  $\sigma$ .

Moreover, since  $\alpha_1 > 0$  and  $\alpha_2 > 0$ , the signs of  $(T - \alpha_1 U_1) \times (\alpha_2 U_2)$ ,  $(\alpha_2 U_1) \times (T - \alpha_2 U_2)$ ,  $T \times (\alpha_2 U_2)$  and  $(\alpha_1 U_1) \times T$  are also  $\sigma$ .

Then  $B$  is convex.

Finally, the curve  $B$  is convex oblique. □

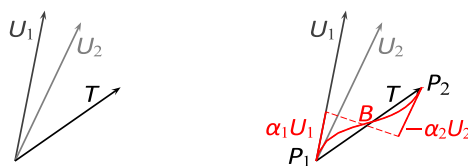


Figure 18: Example of non-degenerate mono-inflective oblique curve, generating set  $S = \{U_1, U_2, T\}$  (left) and generated curve (right)

### $U_1 \times T$ and $T \times U_2$ in opposite sign

Here, a way to generate mono-inflective oblique curves which cross their bases vectors is given.

**Lemma 6.** *Given a set of non-null vectors  $S = \{U_1, U_2, T\}$  in  $\mathbb{R}^2$  such that the subsets  $\{U_1, T\}$  and  $\{U_2, T\}$  are free ( $U_1$  and  $U_2$  can be linearly dependent). Consider that  $T \in \mathbf{Q}_1$  and  $U_1, U_2 \in \overline{\mathbf{Q}}_1$ . Assume that  $U_1 \times T$  and  $T \times U_2$  have opposite signs. Let  $\alpha_1, \alpha_2 \in \mathbb{R}_+^*$ ,  $P_1, P_2 \in \mathbb{R}^2$  be such that  $P_2 = P_1 + T$  and  $B = [P_1, P_1 + \alpha_1 U_1, P_2 - \alpha_2 U_2, P_2]$  the curve generated by  $\{U_1, U_2, T\}$ . The transformation  $\Omega_T$  designates the rectangular inversion of vector  $T$ . Suppose that  $\alpha_1$  and  $\alpha_2$  verify:  $\alpha_1 < \frac{U_2 \times T}{U_1 \times \Omega_T(U_2)}$  and  $\alpha_2 < \frac{U_1 \times T}{U_1 \times \Omega_T(U_2)}$ .*

Then  $B$  is mono-inflective oblique.

*Proof.*

We have that  $T \in \mathbf{Q}_1$  and  $U_1, U_2 \in \overline{\mathbf{Q}}_1$ .

Let  $\Omega_T$  be the rectangular inversion of vector  $T$ .

According to Property 2(3)-(ii),  $\Omega_T(U_2) \in \overline{\mathbf{Q}}_1$ , in addition,  $U_2 \times T$  and  $T \times \Omega_T(U_2)$  are of the same sign.

Hence  $U_1 \times T$  and  $T \times \Omega_T(U_2)$  are of the same sign. Notice that  $T \times \Omega_T(U_2) = U_2 \times T$ .

Let  $\alpha_1 < \frac{T \times \Omega_T(U_2)}{U_1 \times \Omega_T(U_2)}$  and  $\alpha_2 < \frac{U_1 \times T}{U_1 \times \Omega_T(U_2)}$ .

Referring the proof of Lemma 4,  $\alpha_1 U_1$  and  $\alpha_2 \Omega_T(U_2)$  are in  $\mathbf{R}_T$ . Moreover,  $\alpha_1 U_1$  and  $\alpha_2 \Omega_T(U_2)$  are in opposite belonging sign to  $\mathbf{R}_T$ .

By applying Lemma 3, we get that  $[P_1, P_1 + \alpha_1 U_1, P_2 - \Omega_T(\alpha_2 \Omega_T(U_2)), P_2]$  is mono-inflective oblique.  
 But  $\Omega_T(\alpha_2 \Omega_T(U_2)) = \alpha_2 U_2$

Then  $[P_1, P_1 + \alpha_1 U_1, P_2 - \alpha_2 U_2, P_2]$  is mono-inflective oblique. □

Now we'll give a theorem that is a synthesis of the lemmas seen before. Rather, this theorem satisfies the conditions of the lemmas we've seen and allows us to build oblique curves that are either convex or mono-inflective by means of a generating set  $S = \{U_1, U_2, T\}$ . The proof is obvious from the previous results.

**Theorem 2.** Let  $S = \{U_1, U_2, T\}$  a set of non-null vectors in  $\mathbb{R}^2$ . Consider that  $T \in Q_1$  and  $U_1, U_2 \in \overline{Q}_1$ . Let  $\alpha_1, \alpha_2 \in \mathbb{R}_+^*$ ,  $P_1, P_2 \in \mathbb{R}^2$  be such that  $P_2 = P_1 + T$  and  $B = [P_1, P_1 + \alpha_1 U_1, P_2 - \alpha_2 U_2, P_2]$  the curve generated by  $S$ . The transformation  $\Omega_T$  designates the rectangular inversion of vector  $T$ .

- If  $(U_1 \times T)(T \times U_2) > 0$  and

$$\alpha_1 < \frac{T \times U_2}{U_1 \times U_2}$$

$$\alpha_2 < \frac{U_1 \times T}{U_1 \times U_2}$$

then  $B$  is convex oblique.

- If  $(U_1 \times T)(T \times U_2) < 0$  and

$$\alpha_1 < \frac{U_2 \times T}{U_1 \times \Omega_T(U_2)}$$

$$\alpha_2 < \frac{U_1 \times T}{U_1 \times \Omega_T(U_2)}$$

then  $B$  is mono-inflective oblique.

## ALGORITHM

### Oblique sequences of points

We say that a sequence of points  $P = ((x_i, y_i))_{i=0}^n$  in  $\mathbb{R}^2$  is oblique if and only if the sequences  $(x_i)_{i=0}^n$  and  $(y_i)_{i=0}^n$  are strictly monotone (see Figure 19).

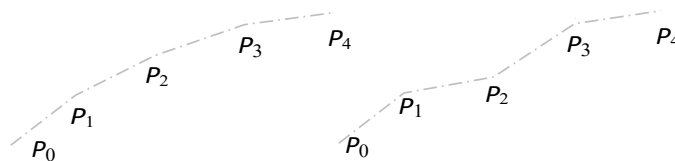


Figure 19: Two oblique sequences of points, convex (left) and non-convex (right).

In the context of this work, a point sequence is said to be non-degenerate when it is not possible to find three or more consecutive points that are collinear.

We say that an ordered sequence of points of  $\mathbb{R}^2$  is *convex* if and only if the polygon with those vertices, in that order, is convex (see Figure 19).

Given an oblique sequence  $\mathbf{P} = (P_i)_{i=0}^n$  in  $\mathbb{R}^2$ , as with BÉZIER curves, we can talk about the notion of type. Referring to Figure 19, the base (or diagonal) of the sequence, i.e. vector  $T = P_n - P_0$ , and  $T_i = P_{i+1} - P_i$  for  $i \in \{0, \dots, n-1\}$  are all in the same quadrant. So the type of the sequence is that of the quarter-plane relative to the quadrant containing the diagonal of the sequence. The sequences in Figure 19 are both of Type  $T_1$  since the bases are in  $Q_1$ .

### Interpolation approach

We continue to carry out the work by considering the quadrant  $Q_1$ . The results obtained remain the same in the other quadrants, with an inversion of direction or sign.

Let  $\mathbf{P} = (P_i)_{i=0}^n$  be the *oblique non-degenerate* sequence of control points to be interpolated. We consider  $n+1$  vectors from the sequence  $\mathbf{V} = (V_i)_{i=0}^n$ , and build an interpolating spline consisting of  $n$  two-dimensional BÉZIER curves from the sequence  $\mathbf{B} = (B_i)_{i=0}^{n-1}$ , where each  $B_i$  starts at  $P_i$  with velocity  $3V_i$  ends at  $P_{i+1}$  with velocity  $3V_{i+1}$ . That is,  $B_i = [P_i, P_i + V_i, P_{i+1} - V_{i+1}, P_{i+1}]$ . Since the arriving and departing velocities are the same at each control point, this construction ensures that the spline is  $C^1$  (continuous in position and velocity).

To carry out the interpolation process for the point sequence  $\mathbf{P}$ , a sequence  $\mathbf{D} = (D_i)_{i=0}^n$  of directions,  $D_i$  is the derivative direction at point  $P_i$ , is required. The aforementioned  $\mathbf{V}$  sequence is defined from the sequence  $\mathbf{D}$ . Note that the vectors of the sequence  $\mathbf{D}$  (and thus those of  $\mathbf{V}$  as we shall see) must be in the same quadrant as the diagonal vector of the sequence to be interpolated, so that the interpolation keeps the obliquity. Three cases concerning the state of  $\mathbf{D}$  are considered in our interpolation approach:

1. The sequence  $\mathbf{D} = (D_i)_{i=0}^n$  is given together with the sequence of points to be interpolated.
2. The directions  $D_0$  and  $D_n$  are given and  $(D_i)_{i=1}^{n-1}$  are to be determined.
3. The entire sequence  $\mathbf{D} = (D_i)_{i=0}^n$  is to be determined.

When the directions are not explicitly given, apart the ones on the boundary points, i.e  $P_0$  and  $P_n$ , the directions are calculated as the mean of the vectors around the point  $P_i$  for  $i = 1, \dots, n-1$ .

Note that the vectors  $\iota = (1, 0)$  and  $\gamma = (0, 1)$  form the orthonormal basis of the plane. Recall that  $T = P_n - P_0$ . The procedure is as follows:

1.  $D_i = \frac{P_{i+1} - P_{i-1}}{2}$ , for  $i \in \{1, \dots, n-1\}$
2. If  $D_0$  is not given then:
 
$$D_0 = \begin{cases} \frac{(P_1 - P_0) + |P_1 - P_0| \cdot \gamma}{2} & \text{if } T \times (P_1 - P_0) > 0 \\ \frac{(P_1 - P_0) + |P_1 - P_0| \cdot \iota}{2} & \text{if } T \times (P_1 - P_0) < 0 \end{cases}$$

3. If  $D_n$  is not given then:

$$D_n = \begin{cases} \frac{(P_n - P_{n-1}) + |P_n - P_{n-1}| \cdot \gamma}{2} & \text{if } T \times (P_n - P_{n-1}) > 0 \\ \frac{(P_n - P_{n-1}) + |P_n - P_{n-1}| \cdot \gamma}{2} & \text{if } T \times (P_n - P_{n-1}) < 0 \end{cases}$$

For  $i$  in  $\{0, 1, \dots, n-1\}$ , let  $T_i$  be the base of  $B_i$ ; that is,  $T_i = P_{i+1} - P_i$ . Then we set  $V_i = h_i D_i$ , for scale factors  $(h_i)_{i=0}^n$  that meet the requirements on Formula (36). The method used to calculate the scale factors sequence  $(h_i)_{i=0}^n$  used to build the directions sequence  $(V_i)_{i=0}^n$  in order to obtain an interpolation of class  $C^1$  is given prematurely but the construction way and useful proof are accomplished in the sequel.

### Construction and proof of the approach

The building and presentation of properties and characteristics, as well as the proof of the interpolation method, is based mainly on the following theorem.

**Theorem 3.** Let  $\mathbf{P} = (P_i)_{i=0}^n$  an oblique non-degenerate sequence of points in  $\mathbb{R}^2$  where the vector  $P_n - P_0$  is in the quadrant  $Q_1$ ,  $\mathbf{D}_P = (D_i)_{i=0}^n$  the sequence of directions and  $\mathbf{T}_P = (T_i)_{i=0}^{n-1}$ ;  $T_i = P_{i+1} - P_i$ , the sequence of bases associated to  $\mathbf{P}$ . Vectors  $D_0, T_0, T_{n-1}$  and  $D_n$  are assumed to be in the same quadrant  $Q_1$ . Consider  $(\alpha_i, \beta_i)_{i=0}^{n-1}$  a sequence in  $\mathbb{R}^* \times \mathbb{R}^*$  and  $\mathbf{B} = (B_i)_{i=0}^{n-1}$  a sequence of BézhXR curves where  $B_i = [P_i, P_i + \alpha_i D_i, P_{i+1} - \beta_i D_{i+1}, P_{i+1}]$ . Assume that  $\alpha_i$  and  $\beta_i$  satisfy what follows:

- If  $(D_i \times T_i)(T_i \times D_{i+1}) > 0$  then
 
$$\alpha_i < \frac{T_i \times D_{i+1}}{D_i \times D_{i+1}}$$

$$\beta_i < \frac{D_i \times T_i}{D_i \times D_{i+1}}$$
- If  $(D_i \times T_i)(T_i \times D_{i+1}) < 0$  then
 
$$\alpha_i < \frac{D_{i+1} \times T_i}{D_i \times \Omega_{T_i}(D_{i+1})}$$

$$\beta_i < \frac{D_i \times T_i}{D_i \times \Omega_{T_i}(D_{i+1})}$$

Then we have:

1.  $\mathbf{B}$  is a  $C^0$  interpolation of  $\mathbf{P}$  based on convex and/or mono-inflective BézhXR curves that are all oblique.
2. If  $\mathbf{P}$  is convex,  $D_i = \frac{P_{i+1} - P_{i-1}}{2}$  for  $i = 1, \dots, n-1$ , and  $D_0 \times T_0, T_0 \times D_1, D_{n-1} \times T_{n-1}$  and  $T_{n-1} \times D_n$  have the same sign, then  $\mathbf{B}$  is a  $C$  convex interpolation of  $\mathbf{P}$  based on oblique convex BézhXR curves.

*Proof.*

When  $D_i = \frac{P_{i+1} - P_{i-1}}{2}$  for  $i = 1, \dots, n-1$ , we can easily prove two results:

1.  $\forall i \in \{1, \dots, n-2\}$ ,  $D_i, T_i$  and  $D_{i+1}$  are in the (same) quadrant  $Q_1$ .

2. When  $\mathbf{P}$  is convex, and  $D_0 \times T_0$ ,  $T_0 \times D_1$ ,  $D_{n-1} \times T_{n-1}$  and  $T_{n-1} \times D_n$  have the same sign, then  $\forall i \in \{1, \dots, n-2\}$ , we get that  $D_i \times T_i$  and  $T_i \times D_{i+1}$  are of the same sign.

Using these two previous results and applying Theorem 2 for each curve  $B_i$ , we prove Theorem 3. □

With applying Theorem 3, we obtain just an interpolation of class  $C^0$ . Indeed, for a point  $P_i, i = 1, \dots, n-1$ , the left and right derivatives are collinear but not necessarily equal. An illustration is given on Figure 20.

To get a  $C^1$  interpolation, the results of Theorem 3 are used. Let  $\mathbf{P} = (P_i)_{i=0}^n$  a convex sequence of points in  $\mathbb{R}^2$ ,  $\mathbf{D_P} = (D_i)_{i=0}^n$  the sequence of directions and  $\mathbf{T_P} = (T_i)_{i=0}^{n-1}$  the sequence of bases associated to  $\mathbf{P}$ . Let  $(\alpha_i, \beta_i)_{i=0}^{n-1}$  be a sequence in  $\mathbb{R}^* \times \mathbb{R}^*$  satisfying Theorem 3.

Consider now the sequence  $(h_i)_{i=0}^n$  in  $\mathbb{R}^*_+$  such that :

$$\begin{cases} h_0 = \alpha_0 \\ h_i < \inf(\beta_{i-1}, \alpha_i), \quad i = 1, \dots, n-1 \\ h_n = \beta_{n-1} \end{cases} \quad (36)$$

Then the sequence of BÉZIER curves  $\mathbf{B} = (B_i)_{i=0}^{n-1}$  where  $B_i = [P_i, P_i + h_i D_i, P_{i+1} - h_{i+1} D_{i+1}, P_{i+1}]$  is an interpolation satisfying the constraints of Theorem 3 but of class  $C^1$ .

The sequences on Figure 20 are reproduced with a  $C^1$  interpolation and presented on Figure 21.

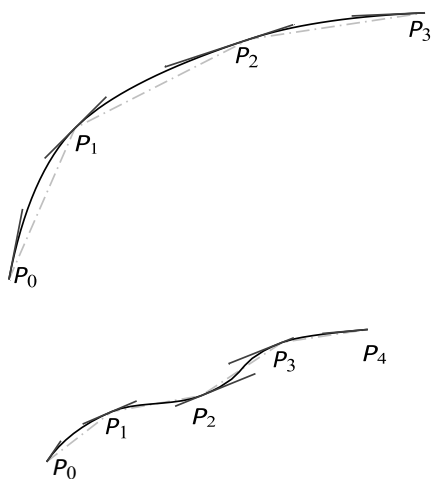


Figure 20:  $C^0$  interpolation of oblique sequences of points, convex (left) non convex (right)

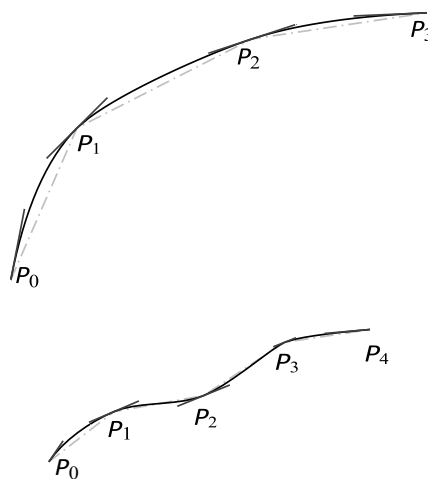


Figure 21:  $C^1$  interpolation of oblique sequences of points, convex (left) non convex (right)

## APPLICATION AND EXAMPLES

As an application, we developed a L<sup>A</sup>T<sub>E</sub>X mini-package that we called meMath and a dynamic font in PostScript Type 3 supporting parenthesis mathematical symbols taking care of optical scaling. Parentheses are implemented on the basis of a set of oblique convex parameterized sequences whose control points are joined by interpolating two-dimensional BÉZIER curves based on our model. We have taken Figure 1 via our package meMath on Figure 22. We can clearly see that the convexity and obliquity characteristics of the top and bottom halves of the contour curves of the parentheses are preserved in both cases.

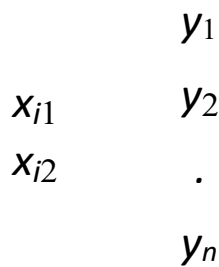


Figure 22: Parentheses (delimiters) as dynamic symbols with meMath

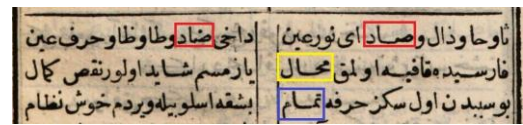


Figure 23: Justification in Arabic Scripts with Kashida

To show how our research work is applied to support the justification of Arabic texts, we consider Figure 23 which is referenced in [15]. This is a text in Arabic letters taken from an old book. It’s presented in two justified columns. Justification is not achieved by inserting blank spaces, as is the case with Latin text, but by letting letters undergo curvilinear stretching. This mechanism, in Arabic calligraphic rules, is called Kashida. All Framed words in the right column are stretched cases of some Arabic words. The color differences in framing mean (for those who don’t read Arabic) that these are different words. The words framed in red are used to highlight the concept. The characters H and N are two Arabic letters called respectively Sad and Dad. They undergo the same rules in writing. They differ only by the top diacritic point. Also, their names in Arabic, **ﺩ** (Sad) and **ﺪ** (Dad), are written in the same way, they respect the same rules in stretching and are distinguished only by a top diacritic point. Basically, the red framed word in the right column (Sad) is a stretched version of the red framed one in the left (Dad minus the diacritic point). We developed, based on our mathematical algorithm, a PostScript mini-font Type 3 “naskh” that support stretching of Arabic writing. **ﺩ** is a stretched state of **ﺪ** by an amount of 6 diacritic point horizontally and a quarter of diacritic point vertically (down) using “naskh” at 14pt size.

### CONCLUSIONS AND PERSPECTIVES

We have developed an approach for interpolating a non-degenerate oblique sequence of points by a sequence of cubic BÉZIER curves, preserving both convexity, inflection and obliquity. The interpolation approach is based on oblique convex BÉZIER curves and oblique mono-inflective cubic BÉZIER curves crossing their bases.

An intuitive extension of the interpolation method developed in this paper is to provide support for

degenerate oblique sequences. Another interesting extension is to improve the method so that we can interpolate sequences of points that may or may not be oblique, while still using convex and mono-inflective oblique BÉZIER curves.

For our purposes and applications,  $C^1$  continuity was all we needed. In other areas, geometric continuity is of great interest. The method will be extended to take into account geometric continuity.

## References

- [1] Systems Incorporated Adobe. *Adobe Type 1 Font Format*. Addison-Wesley Publishing Company, Inc, United States of America, 3th edition, 1993.
- [2] Amine Anane. Arabic text justification using LuaL<sup>A</sup>T<sub>E</sub>X and the digitalkhatt opentype variable font. *TUGboat*, 42(3):247–257, 2021.
- [3] Abdelouahad Bayar.  $C^1$  interpolation of sequences of points preserving convexity and obliquity based on oblique convex two-dimensional cubic Bézier splines. In *2024 IEEE International Conference on Signal, Image, Video and Communications (ISIVC 2024)*, pages 1–6, Marrakech, Morocco, May 2024.
- [4] Abdelouahad Bayar and Khalid Sami. Stretching of dynamic mathematical symbols taking care of similarity and geometric characterization. *Mathematical Problems in Engineering*, 2017:13, 2017.
- [5] M. J.E. Benatia, M. Elyaakoubi, and A. Lazrek. Arabic text justification. In *TUGboat, Volume 27 (2006), No. 2 - Proceedings of the 2006 Annual Meeting*, volume 27, pages 137–146, Marrakesh, Morocco, 2006.
- [6] V. V. Borisenko. Construction of optimal Bézier splines. *Journal of Mathematical Sciences*, 237(3):375–386, 2019.
- [7] Carl De Boor. *A practical guide to splines*. Applied mathematical sciences. Springer-Verlag, New York, NY, 1st edition, 1978.
- [8] Randall L. Dougherty, Alan S. Edelman, and James M. Hyman. Nonnegativity-, monotonicity-, or convexity-preserving cubic and quintic hermite interpolation. *Mathematics of Computation*, 52(186):471–494, 1989.
- [9] F. N. Fritsch and R. E. Carlson. Monotone piecewise cubic interpolation. *SIAM Journal on Numerical Analysis*, 17(2):238–246, 1980.
- [10] André Jacques and Vatton Irène. Dynamic optical scaling and variable-sized characters. *Electron. Publ.*, 7(4):231–250, 1994.
- [11] Deok-Soo Kim. Hodograph approach to geometric characterization of parametric cubic curves. *Computer-Aided Design*, 25(10):644–654, 1993.
- [12] Gary D. Knott. *Cubic Spline Vector Space Basis Functions*, pages 143–155. Birkhäuser Boston, Boston, MA, 2000.
- [13] Marcel Krüger. Metapost-based, dynamic extensible delimiters for LuaT<sub>E</sub>X. In *TUGboat'2020, The 41<sup>th</sup> Annual Meeting of the TeX Users Group*, volume 41, Online, 2020.

- [14] Azzeddine Lazrek. Curext, typesetting variable-sized curved symbols. In *TUGboat, Volume 24 (2003), No. 3 - Proceedings of EuroTEX 2003 : 14th. European TeX conference*, volume 24, pages 323–327, Brest, France, 2003.
- [15] Titus Nemeth. On arabic justification. *The journal electronic publishing*, 23(1), 2020.
- [16] Southall Richard. Character description techniques in type manufacture. In *RIDT 91: Conference proceedings on Raster imaging and digital typography II*, pages 16–27. Cambridge University Press, 40 W. 20 St. New York, NY United States, 1991.
- [17] José A. Ruiz-Arias. Mean-preserving interpolation with splines for solar radiation modeling. *Solar Energy*, 248:121–127, 2022.
- [18] Lejun Shao and Hao Zhou. Curve fitting with Bézier cubics. *Graphical Models and Image Processing*, 58(3):223–232, 1996.
- [19] Ameer M. Sherif and Hossam A. H. Fahmy. Parameterized arabic font development for alqalam. In *TUGboat, Volume 29, No. 1 - XVII European TEX Conference, 2007*, volume 29, pages 79–88, Bachotek, Poland, 2008.
- [20] Helmuth Späth. *One Dimensional Spline Interpolation Algorithms*. A K Peters/CRC Press, New York, 1st edition, 1995.
- [21] Maureen Stone and Tonu DeRose. A geometric characterization of parametric cubic curves. *ACM Transactions on Graphics*, 8(3):147–163, 1989.
- [22] Buchin Su and Dingyuan Liu. An affine invariant theory and its application in computational geometry. *Science in China Series A-Mathematics, Physics, Astronomy & Technological Science*, 26(3):259–272, 1983.
- [23] Meng Sun, Lin Lan, Chun-Gang Zhu, and Fengchun Lei. Cubic spline interpolation with optimal end conditions. *Journal of Computational and Applied Mathematics*, 425:115039, 2023.
- [24] C. Y. Wang. Shape classification of the parametric cubic curve and parametric b-spline cubic curve. *Computer-Aided Design*, 13(4):199–206, 1981.
- [25] D. Weise and D. Adler. Truetype and microsoft windows 3.1. Technical report, Microsoft Corporation, 1992.